International Journal of Computer Information Systems and Industrial Management Applications
ISSN 2150-7988 Volume 18(9s) 2026 pp. 496-529
https://doi.org/10.70917/ijcisim-2026-3454
Article

"Exploration of Mathematical Constructs in Fourier Transform Techniques for Biomedical Signal Interpretation"

Shital R. Shinde[1], Anil Agrawal[2]

[1]Department of Mathematics, Sage University, Indore (M.P) Maharashtra, 452020, India
[2] Department of Mathematics, Sage University, Indore (M.P) Maharashtra, 452020, India

Abstract: This study introduces a comprehensive mathematical framework for Fourier transform-based analysis of biomedical signals including ECG, EEG, and EMG, addressing the limitations of traditional time-domain methods in capturing frequency-domain physiological signatures essential for early diagnosis of cardiovascular, neurological, and neuromuscular disorders. Methodologically, it derives explicit analytical expressions for continuous-time Fourier transform (CTFT), discrete-time Fourier transform (DTFT), discrete Fourier transform (DFT), short-time Fourier transform (STFT), and spectrograms tailored to bio signal characteristics, encompassing ECG P-QRS-T spectral modeling (5–50 Hz bands), EEG canonical band powers (delta 0.5–4 Hz to gamma 30–100 Hz), EMG mean/median frequencies (MNF/MDF), noise models (baseline wander 0.05–0.5 Hz, powerline 50/60 Hz), and time–frequency representations for non-stationary analysis. The proposed work establishes a modular processing pipeline with standardized preprocessing (anti-aliasing, windowing via Hann/Hamming/Blackman), feature extraction (PSD via Welch's method, spectral moments, spectro-temporal metrics), and validation on benchmark datasets, enabling seamless integration with machine learning classifiers for tasks like arrhythmia detection, seizure identification, and fatigue assessment. Expected outcomes include improved diagnostic accuracy through interpretable frequency-domain biomarkers, a reusable library of mathematical formulations for reproducible research, enhanced real-time monitoring capabilities for wearables, and foundational advancements toward hybrid AI-time-frequency models that bridge classical signal processing with modern deep learning paradigms.

Keywords: Convolutional Neural Network**,** EEG Spectral Bands, EMG Frequency Features, Short-Time Fourier Transform (STFT), Spectrogram, Power Spectral Density (PSD), Time-Frequency Analysis, Frequency-Domain Features,

1. Introduction

Fourier-based analysis provides a mathematical framework to decompose complex biomedical signals, such as ECG, EEG and EMG, into constituent frequency components that reveal physiological rhythms and pathological patterns not easily visible in the time domain. In modern biomedical engineering, these tools underpin diagnostic, monitoring and decision-support systems used across cardiology, neurology and critical care.

1.1 Background of biomedical signal processing

Biomedical signal processing deals with the acquisition, enhancement, analysis and interpretation of physiological signals generated by the cardiovascular, neural, muscular and other organ systems, including ECG, EEG, EMG, PCG and PPG. Early work focused on analog filtering and simple feature extraction, but digital signal processing, transform-based methods and machine learning have enabled more precise characterization of rhythms, morphologies and noise in clinical and wearable-monitoring settings (Challis & Kitney, 1991; Gómez-Echavarría et al., 2020). Biomedical signals are often low amplitude, contaminated by artifacts (motion, Signal-line interference, baseline wander) and subject-specific, so robust preprocessing, denoising and feature-extraction pipelines are essential before higher-level analysis and classification (Challis & Kitney, 1991; Khandpur, 2014).

1.2 Importance of frequency-domain analysis

Frequency-domain analysis transforms time-series signals into spectra that describe how Signals are distributed over frequency, allowing identification of dominant bands, harmonics and periodicities. In practice, spectral features such as band Signals, peak frequencies and bandwidths are widely used to quantify brain rhythms in EEG (delta, theta, alpha, beta, gamma), assess muscle fatigue in EMG, and analyze HRV components in ECG for autonomic balance, stress and emotion assessment (Shen et al., 2013; Vieira et al., 2024). Frequency-domain methods also play a key role in diagnostic tasks, for example detecting arrhythmia-related spectral signatures in ECG or seizure-related changes in EEG, and in designing digital filters to remove narrowband noise such as Signal-line interference (Wang et al., 2024).

1.3 Role of mathematical expressions in Fourier transform

Fourier analysis represents a signal as a weighted sum or integral of complex exponentials, with the Fourier series and Fourier transform expressed through well-defined integrals and summations that rigorously link time-domain signals $x(t)$ or $x[n]$ to their spectra $X(f)$ or $X(k)$.

In biomedical applications, these mathematical expressions underpin discrete Fourier transform (DFT) and fast Fourier transform (FFT) algorithms, enabling efficient computation of Signal spectral density, coherence, cross-spectra and frequency-domain filters used for noise suppression, feature extraction and connectivity analysis (Gómez-Echavarría et al., 2020; Oppenheim & Schafer, 2010). Extensions such as the fractional Fourier transform and generalized integral transforms rely on modified kernel expressions to provide intermediate domains between time and frequency, improving analysis of chirp-like or dispersive biomedical signals (Gómez-Echavarría et al., 2020; Gupta & Sahu, 2025).

In modern healthcare systems Biomedical signal processing has emerged as a fundamental discipline bridging classical signal theory with clinical applications. Biomedical signals such as ECG, EEG, and EMG are inherently analog physiological measurements that is converted into digital form for computational analysis and feature extraction. These signals contain diagnostic information that is often difficult to discern in their raw time-domain representation, necessitating sophisticated signal processing methodologies to extract clinically meaningful features. The complexity of these signals arises from their non-stationary nature—the frequency content changes over time—combined with the presence of multiple noise sources including baseline wander, Signal-line interference, motion artifacts, and environmental electromagnetic interference.[1][2][3][4][5][6]

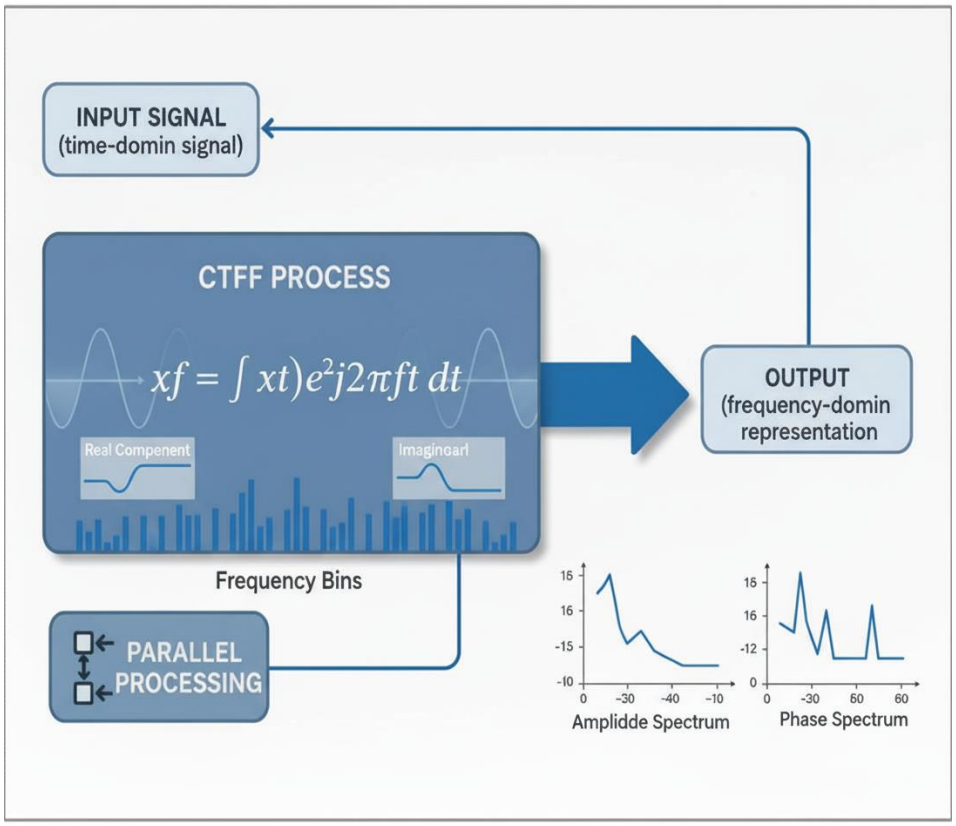

Figure 1: Fig1: Continuous-Time Fourier Transform (CTFT) Process and Mathematical Formulation

Frequency-domain analysis provides complementary insights to time-domain observations, revealing the spectral composition of biomedical signals that constitute their essential diagnostic characteristics. In the frequency domain, characteristic patterns emerge that differentiate normal physiological states from pathological conditions: for example, abnormal QRS complexes in cardiac arrhythmias exhibit distinct frequency signatures, while epileptic seizures produce characteristic changes in EEG spectral content. The Fourier-based approach decomposes complex time-varying signals into constituent sinusoidal components, each characterized by specific amplitude and phase values, enabling targeted filter design, noise removal, and feature-based classification. This transformation permits the application of classical control theory, adaptive filtering algorithms, and spectral estimation methods that have become indispensable in modern diagnostic systems and real-time patient monitoring applications.[1][7][8][9][10][11][12]

The mathematical formulation of Fourier transforms provides the theoretical foundation for converting biomedical signals between time and frequency domains with rigorous quantification of energy distribution, spectral components, and temporal localization. Mathematical expressions enable precise characterization of signal properties such as bandwidth, harmonic content, and time-frequency resolution trade-offs that directly impact the design of diagnostic algorithms and sensor specifications. The Euler formula and complex exponential representation form the mathematical basis for understanding phase relationships and coherence measurements between different signal channels, critical for applications like localizing neuronal sources in EEG analysis or detecting synchronization abnormalities in cardiac signals.[13][14][10][6]

1.4 Challenges in analyzing non-stationary biomedical signals

[1,2,8,9]. [15][5][16][14][17][18]

A major limitation of the classical Fourier transform is its global nature, which assumes stationarity over the analysis window and therefore cannot track rapid temporal evolution in signals whose frequency content changes over time, such as transient ECG ischemic events, epileptic seizures in EEG or muscle activation bursts in EMG. Non-stationary biomedical signals require joint time–frequency representations, but methods like short-time Fourier transform (STFT) face an inherent trade-off between time and frequency resolution due to fixed window length, while wavelet-based approaches, although offering multiresolution analysis, must carefully choose mother wavelets and parameters to balance sensitivity, robustness and computational cost (Akhtar & Kumar, 2024). Additional challenges include inter-subject variability, low SNR, motion artifacts and real-time constraints in wearable and IoT settings, which complicate the design of adaptive, mathematically rigorous time–frequency algorithms for clinical deployment (Daqrouq et al., 2023; Kumar et al., 2025).

2.1 Definition and mathematical formulation

2.1.1 Continuous-time Fourier transform (CTFT)

For an aperiodic continuous-time signal $x(t)$ with suitable integrability conditions, the CTFT is

$$X(f) = \int_{-\infty}^{\infty} x(t)\ e^{-j2\pi ft}\, dt$$

and the inverse transform is

$$x(t) = \int_{-\infty}^{\infty} X(f)\ e^{j2\pi ft}\, df.$$

These expressions map a time-domain waveform into a continuous frequency-domain spectrum and back, and form the basis for continuous-time spectral analysis in biomedical applications such as ECG and EEG filtering and interpretation.

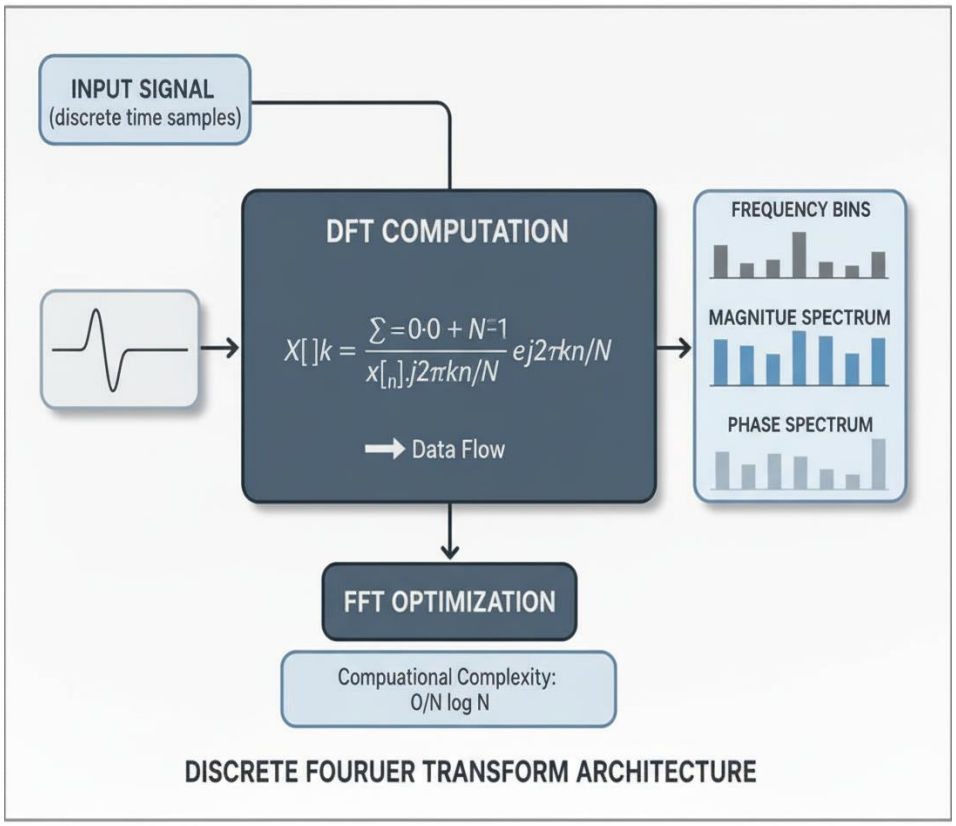

Figure 2: Fig2: Discrete Fourier Transform (DFT) and FFT Computational Framework

2.1.2 Discrete-time Fourier transform (DTFT)

For a discrete-time sequence $x[n]$ defined for all integer n, the DTFT is

$$X(e^{j\omega}) = \sum_{n=-\infty}^{\infty} x[n]\ e^{-j\omega n} \quad \ldots\ldots\ldots\ldots\ldots\ldots [1]$$

$$X[k] = \sum_{n=0}^{N-1} x[n]\ e^{-j\frac{2\pi}{N}kn}, k = 0,1, \ldots, N-1$$

with inverse

$$x[n] = \frac{1}{2\pi}\int_{-\pi}^{\pi} X(e^{j\omega})\, e^{j\omega n}\, d\omega. \quad \ldots \qquad \ldots\ldots\ldots [2]$$

The DTFT produces a 2π-periodic continuous function of angular frequency ω, and is central for analyzing digital filters and sampled biomedical signals prior to numerical approximation via the discrete Fourier transform.

2.1.3 Discrete Fourier transform (DFT)

For a finite-length sequence $x[n]$, $n = 0,1,\dots,N-1$, the N-point DFT is

$$Xk=n=0N\text{-}1xn\ e\text{-}j2\pi Nkn,k=0,1,\dots,N\text{-}1$$

with inverse

$$x[n] = \frac{1}{N}\sum_{k=0}^{N-1} X[k]\ \ e^{j\frac{2\pi}{N}kn}, n = 0,1,\dots,N-1.$$

The DFT samples the DTFT on a uniform frequency grid and is implemented efficiently by the FFT, making it the workhorse for spectral estimation, HRV analysis, EMG fatigue assessment and EEG band-Signal computation in biomedical signal processing.

2.2 Complex exponential representation

A key idea in Fourier analysis is that sinusoids can be represented as sums of complex exponentials using Euler's formula,

$$e^{j\theta} = \cos\theta + \mathrm{j}\sin\theta\,.$$

Any finite-energy signal can be decomposed into a superposition (integral or sum) of complex exponentials $e^{j2\pi ft}$ or $e^{j\omega n}$, where the Fourier transform provides the complex weights $X(f)$ or $X\left(e^{j\omega}\right)$.

For example, a real sinusoid can be written as

$$\cos(2\pi f_0 t) = \frac{1}{2}\left(e^{j2\pi f_0 t}+e^{-j2\pi f_0 t}\right),$$

demonstrating that frequency-domain analysis effectively measures how much of each complex exponential basis function is present in a biomedical signal.

2.3 Properties of Fourier transform

2.3.1 Linearity

If $x_1(t) \leftrightarrow X_1(f)$ and $x_2(t) \leftrightarrow X_2(f)$ under the CTFT, then for any constants a and b,

$$a\,x_1(t) + b\,x_2(t)\ \ \leftrightarrow\ \ a\,X_1(f) + b\,X_2(f).$$

An analogous property holds for DTFT and DFT. Linearity allows biomedical engineers to analyze composite signals—such as ECG plus noise—as sums of simpler components, and to design filters by superimposing responses.

2.3.2 Time and frequency shifting

For CTFT, a time shift $x(t - t_0)$ produces a linear phase term in the spectrum:

$$x(t - t_0)\ \ \leftrightarrow\ \ X(f)\,e^{-j2\pi f t_0}.$$

Conversely, modulation (frequency shift) by a complex exponential leads to a spectral shift:

$$x(t)\,e^{j2\pi f_0 t}\ \ \leftrightarrow\ \ X(f - f_0).$$

Similar relations hold for discrete-time signals with $e^{-j\omega n_0}$ factors and circular frequency shifts in the DFT. Time–frequency shifting properties are used to model delays in physiological systems, analyze phase responses of filters and implement frequency-translation operations in bio-signal processing.

2.3.3 Convolution theorem

If $y(t) = x(t) * h(t) = \int_{-\infty}^{\infty} x(\tau)h(t-\tau)\,d\tau$, then

$$y(t) = x(t) * h(t) \;\leftrightarrow\; Y(f) = X(f)\,H(f).$$

In discrete time,

$$y[n] = \sum_{m=-\infty}^{\infty} x[m]\,h[n-m] \;\leftrightarrow\; Y(e^{j\omega}) = X(e^{j\omega})\,H(e^{j\omega}),$$

and for the DFT the linear convolution (with appropriate zero-padding) corresponds to pointwise multiplication in the frequency domain. This theorem underlies frequency-domain filter design and efficient FFT-based convolution used for ECG baseline wander removal, EMG smoothing and EEG band-pass filtering.

2.3.4 Parseval's theorem

For CTFT, Parseval's theorem states that total signal energy in time equals energy in frequency:

$$\int_{-\infty}^{\infty} |\,x(t)\,|^2\;dt = \int_{-\infty}^{\infty} |\,X(f)\,|^2\;df.$$

For discrete-time sequences, the DTFT form is

$$\sum_{n=-\infty}^{\infty} |\,x[n]\,|^2 = \frac{1}{2\pi}\int_{-\pi}^{\pi} |\,X(e^{j\omega})\,|^2\;d\omega,$$

and the N-point DFT version is

$$\sum_{n=0}^{N-1} |\,x[n]\,|^2 = \frac{1}{N}\sum_{k=0}^{N-1} |\,X[k]\,|^2.$$

These identities justify computing signal Signal and band-limited energies from spectral coefficients, which is crucial for HRV Signal analysis, EEG band-Signal metrics and EMG energy-based fatigue indices.

2.4 Sampling theory and aliasing

2.4.1 Nyquist criterion

For a band-limited continuous-time signal with maximum frequency $f_{\max}$, the Nyquist–Shannon sampling theorem states that perfect reconstruction from uniform samples with sampling frequency f_s is possible if

$$f_s \geq 2f_{\max}.$$

Equivalently, the sampling interval must satisfy $T_s \leq \frac{1}{2f_{\max}}$.

If $f_s < 2f_{\max}$, higher-frequency components fold (alias) into lower frequencies, distorting the spectrum and potentially corrupting biomedical interpretations (e.g., spurious low-frequency components in ECG or EEG).

2.4.2 Anti-aliasing filters

In practical data acquisition, many biomedical signals are not strictly band-limited, so an analog low-pass anti-aliasing filter with cutoff f_c slightly below $\frac{f_s}{2}$ is applied before sampling. Ideal anti-aliasing would use a brick-wall low-pass response with gain 1 ~~form~~ ~~1~~ for $|f| \leq f_c$ and 0 otherwise, but realizable circuits approximate this response while balancing transition-band width and phase distortion. Proper anti-aliasing design ensures that spectral estimates from sampled ECG, EEG and EMG accurately reflect true physiological content without contamination from aliased high-frequency noise.

Commented [1]:

2.5 Windowing Functions

2.5.1 Hamming, Hanning, Blackman

When computing the DFT of finite records, window functions $w[n]$ taper the data to reduce discontinuities at the boundaries and control spectral leakage. For an N-point sequence, common windows include:

- Hann (Hanning) window

$$w_{\text{Hann}}[n] = 0.5 - 0.5\cos\left(\frac{2\pi n}{N-1}\right), 0 \leq n \leq N-1.$$

- Hamming window

$$w_{\text{Hamming}}[n] = 0.54 - 0.46\cos\left(\frac{2\pi n}{N-1}\right), 0 \leq n \leq N-1.$$

- Blackman window

$$w_{\text{Blackman}}[n] = 0.42 - 0.5\cos\left(\frac{2\pi n}{N-1}\right) + 0.08\cos\left(\frac{4\pi n}{N-1}\right), 0 \leq n \leq N-1.$$

These windows differ in main-lobe width and side-lobe attenuation: Hann provides moderate leakage suppression, Hamming offers better side-lobe reduction, and Blackman further suppresses side-lobes at the cost of wider main lobes. In biomedical spectrum estimation, window choice trades frequency resolution against leakage when analyzing narrowband rhythms or closely spaced spectral components.

2.5.2 Spectral leakage and resolution

Multiplying a finite-length signal segment by a window corresponds in the frequency domain to convolving the signal's true spectrum with the window's spectral response, which causes spectral leakage when energy from a tone spread into neighbouring frequency bins. Narrow main lobes improve frequency resolution (ability to distinguish close tones), whereas low side-lobes reduce leakage but broaden the main lobe; thus, the choice of window and record length N jointly determines the trade-off between resolving Signal and leakage in biomedical spectral analysis. For example, long Hann- or Blackman-windowed segments can resolve small shifts in dominant EEG bands or subtle EMG spectral changes, whereas shorter windows improve temporal tracking at the expense of frequency precision.

3.1 Mathematical expression of ECG in frequency domain

A single-lead ECG signal $x_{\text{ECG}}(t)$ can be modelled as a sum of its main morphological components (P-wave, QRS complex and T-wave) plus noise:

$$x_{\text{ECG}}(t) = p(t) + qrs(t) + t_w(t) + n(t),$$

where $n(t)$ aggregates baseline wander, Signal-line interference and other artifacts. Taking the continuous-time Fourier transform (CTFT),

$$X_{\text{ECG}}(f) = P(f) + QRS(f) + T_w(f) + N(f),$$

with each term capturing the specific spectral content of the corresponding waveform. Typical clinical bands for normal ECG waves are approximately 5–30 Hz for P-wave, 8–50 Hz for QRS, and 0.5–10 Hz for T-wave, so ideal band-pass filters for delineation are often chosen to emphasize these bands and attenuate others. –

3.1.1 FT of P-wave, QRS complex, T-wave

Analytically, each wave can be approximated by simple parametric forms whose Fourier transforms are known in closed form. For example, a P-wave can be modelled as a Gaussian pulse

$$p(t) = A_p \exp\left(-\frac{(t-t_p)^2}{2\sigma_p^2} \right),$$

whose FT is

$$P(f) = A_p \sigma_p \sqrt{2\pi} \exp\left(-2\pi^2 \sigma_p^2 f^2 \right) e^{-j2\pi f t_p},$$

yielding a smooth low-pass spectrum aligned with its reported 5–30 Hz band. The QRS complex, being much sharper, is often represented by a sum of Gaussians or derivatives of Gaussians, such as

$$qrs(t) = \sum_{k=1}^{K} A_k \exp\left(-\frac{(t-t_k)^2}{2\sigma_k^2} \right),$$

leading to

$$QRS(f) = \sum_{k=1}^{K} A_k \sigma_k \sqrt{2\pi} \exp\left(-2\pi^2 \sigma_k^2 f^2 \right) e^{-j2\pi f t_k},$$

with relatively broader spectra up to 40–50 Hz in normal conduction and extending beyond 70 Hz in abnormal ventricular conduction. The T-wave can be modelled as a wider, lower-frequency Gaussian-like pulse, producing dominant spectral energy below about 10 Hz and capturing repolarization dynamics.

3.1.2 Noise modeling (baseline wander, Signal-line noise)

Baseline wander is typically modelled as a very-low-frequency component arising from respiration and electrode motion, e.g.

$$n_{\mathrm{BW}}(t) = A_b \sin(2\pi f_b t + \phi_b),$$

with f_b in the range 0.05–0.5 Hz; its FT consists of impulses at $\pm f_b$, allowing high-pass filters with cut-off around 0.5 Hz to suppress this artifact. Signal-line interference is usually represented as

$$n_{\mathrm{PL}}(t) = A_p \sin\left(2\pi f_p t + \phi_p\right),$$

with $f_p = 50$ or 60 Hz depending on the mains frequency, producing narrow spectral lines at $\pm f_p$ that motivate notch filters centered at 50/60 Hz. The overall ECG noise spectrum can be modeled as

$$N(f) = N_{BW}(f) + N_{PL}(f) + N_{HF}(f),$$

where $N_{\mathrm{HF}}(f)$ accounts for muscle and instrumentation noise with broader, often approximately white or $\frac{1}{f}$ characteristics. –

3.2 Mathematical expression for EEG spectral components

A multichannel EEG signal $x_c(t)$ at channel c is commonly analyzed via its Signal spectral density (PSD) to quantify standard frequency bands: delta (≈0.5–4 Hz), theta (≈4–8 Hz), alpha (≈8–13 Hz), beta (≈13–30 Hz) and gamma (≈30–100 Hz). Let $X_c(f)$ be the Fourier transform of the windowed EEG segment; then the band Signal for a band $B = [f_1, f_2]$ is

$$P_c(B) = \int_{f_1}^{f_2} | X_c(f) |^2 \ df$$

for a continuous spectrum, or for a sampled spectrum with resolution Δf,

$$P_c(B) \approx \sum_{f_k \in B} | X_c(f_k) |^2 \ \Delta f . [\ \ ][\ \ ]$$

Normalized band Signals $\frac{P_c(B)}{\sum_{B'} P_c(B')}$ are often used to express the relative contribution of each band to total EEG Signal.

3.2.1 Delta, theta, alpha, beta, gamma bands

For a sampling frequency f_s, frequency bins in the DFT are $f_k = \frac{k f_s}{N}$, and band Signals are computed by summing squared magnitudes over the indices corresponding to each canonical band. For example, the alpha-band Signal for channel c in a window of length N is

$$P_c^{\alpha} = \sum_{k:\,8\text{ Hz} \le f_k \le 13\text{ Hz}} | X_c[k] |^2,$$

and analogous formulas define $P_c^{\delta}, P_c^{\theta}, P_c^{\beta}, P_c^{\gamma}$. Empirically, resting-state EEG often shows dominant theta and alpha PSD during baseline, while cognitive tasks shift Signal toward beta and gamma bands. –

3.2.2 PSD formulation for brain activity

A widely used PSD estimator is Welch's method, which averages modified periodograms over overlapping windows. If a signal is divided into M segments $x_m[n]$ (each windowed by $w[n]$), the Welch PSD estimate is

$$\hat{S}_{xx}(f) = \frac{1}{MUf_s} \sum_{m=1}^{M} | \sum_{n=0}^{N-1} x_m [n] \, w[n] \, e^{-\frac{j2\pi f n}{f_s}} |^2 ,$$

where $U = \frac{1}{N} \sum_{n=0}^{N-1} w^2 [n]$ normalizes for window energy. Band-limited PSD values $\hat{S}_{xx}(f)$ integrated over canonical bands provide quantitative markers of cortical activation, workload, sleep stages and pathological activity such as seizures or encephalopathy. –

3.3 EMG frequency-domain modeling

Surface EMG signals reflect the superposition of motor unit action potentials and are often modelled by their Signal spectra for fatigue and force estimation. Let $S_{\text{EMG}}(f)$ denote the EMG PSD; global features such as mean frequency (MNF) and median frequency (MDF) summarize how spectral energy distributes over the analysis band $[f_{\text{min}}, f_{\text{max}}]$.

3.3.1 Mean frequency (MNF)

The mean frequency is defined as the first spectral moment normalized by total Signal:

$$\text{MNF} = \frac{\int_{f_{\min}}^{f_{\max}} f \; S_{\text{EMG}}(f)\, df}{\int_{f_{\min}}^{f_{\max}} S_{\text{EMG}}(f)\, df},$$

or in discrete form,

$$\text{MNF} = \frac{\sum_{k=k_{\min}}^{k_{\max}} f_k \; S_{\text{EMG}}(f_k)}{\sum_{k=k_{\min}}^{k_{\max}} S_{\text{EMG}}(f_k)}.$$

During sustained isometric contractions, MNF typically shifts to lower frequencies as muscle fatigue develops, reflecting changes in conduction velocity and motor unit recruitment.

3.3.2 Median frequency (MDF)

The median frequency is the frequency that divides the total spectral Signal into two equal halves:

$$\int_{f_{\min}}^{\text{MDF}} S_{\text{EMG}}(f)\, df = \frac{1}{2}\int_{f_{\min}}^{f_{\max}} S_{\text{EMG}}(f)\, df.$$

In discrete form, MDF is the smallest f_k such that

$$\sum_{i=k_{\min}}^{k} S_{\text{EMG}}(f_i) \;\geq\; \frac{1}{2}\sum_{i=k_{\min}}^{k_{\max}} S_{\text{EMG}}(f_i).$$

Both MNF and MDF decrease with increasing fatigue in many muscles, and time-varying MNF/MDF trajectories (TD-MNF, TD-MDF) have been proposed as robust fatigue indices in dynamic contractions.

3.4 Analytical expressions for time–frequency transform

3.4.1 Short-time Fourier transform (STFT) equation

To handle non-stationary biomedical signals such as ECG with transient ischemic changes, EEG with bursts or EMG with activation onsets, the short-time Fourier transform (STFT) analyzes local frequency content using a sliding window. The continuous-time STFT of a signal $x(t)$ with analysis window $w(t)$ is

$$X(t,f) = \int_{-\infty}^{\infty} x(\tau)\, w(\tau - t)\; e^{-j2\pi f\tau}\, d\tau,$$

while the discrete-time version is

$$X[m,k] = \sum_{n=-\infty}^{\infty} x[n]\; w[n-m]\; e^{-\frac{j2\pi kn}{N}},$$

where m indexes time frames and k frequency bins. Proper choice of window length and overlap controls the trade-off between time and frequency resolution, which is critical for capturing rapid events such as QRS complexes or epileptiform spikes.

3.4.2 Spectrogram formation

The spectrogram is defined as the squared magnitude of the STFT,

$$Spec(t,f) = |X(t,f)|^2,$$

or in discrete form $\text{Spec}[m,k] = |X[m,k]|^2$, often displayed as a color map with time on the horizontal axis, frequency on the vertical axis and color indicating Signal. In ECG analysis, spectrograms can reveal frequency evolution across P–QRS–T cycles; in EEG they highlight transient bursts in specific bands, and in EMG they show how spectral energy migrates to lower frequencies as fatigue develops. Time–frequency energy measures derived from the spectrogram, such as band-limited integrated Signal over time, offer richer descriptors than purely time- or frequency-domain metrics for complex biomedical signals.

Motivation for this study arises from the growing need to move beyond purely time-domain inspection of ECG, EEG and EMG toward rigorous mathematical modeling that can expose subtle pathological patterns at an early and clinically actionable stage (Rajeswari et al., 2017; Sandsten, 2013). Traditional visual interpretation by clinicians is time-consuming and subjective, and it often fails to capture complex, multi-component and non-stationary characteristics of bio signals that are better described through Fourier and time–frequency–based mathematical expressions (Mahmoud et al., 2006; Senay et al., 2018). Developing a unified framework of mathematical expressions for frequency-domain and time–frequency analysis of ECG, EEG and EMG can therefore support robust feature extraction, automated classification and integration with machine-learning models for diagnosis and monitoring (Raez et al., 2006; Duhan et al., 2011; Wang et al., 2024).

The significance of the study lies in its potential to improve diagnostic accuracy, early detection and quantitative monitoring of cardiovascular, neurological and neuromuscular disorders by exploiting frequency-domain and time–frequency biomarkers (Rajeswari et al., 2017; Vallat, 2019). For example, ECG frequency features can enhance arrhythmia and ischemia detection, qEEG spectral indices can provide objective markers for dementia and epilepsy, and EMG spectral shifts can quantify muscle fatigue and rehabilitation progress (Mahmoud et al., 2006; Raez et al., 2006; Senay et al., 2018). By formalizing mathematical expressions for band Signals, Signal spectral density, mean and median frequencies, and time–frequency representations, the study creates a reproducible foundation that can be directly embedded into computer-aided diagnosis and clinical decision-support systems (Mahmoud et al., 2006; Al-Jobouri & Al-Ani, 2015; Vallat, 2019).

The need for this study is further reinforced by the intrinsic non-stationarity and multicomponent nature of biomedical signals, which violates the assumptions of classical stationary Fourier analysis and demands high-resolution time–frequency techniques (Hosseini et al., 2017; Sandsten, 2013). ECG, EEG and EMG often exhibit transient bursts, frequency drifts and overlapping components, so inadequate mathematical modeling can lead to misinterpretation of subtle pathological changes or failure to detect early disease markers (Mahmoud et al., 2006; Senay et al., 2018). Systematically deriving and organizing mathematical expressions for Fourier, short-time Fourier and related transforms tailored to bio signals will help address current gaps in standardization, reproducibility and interpretability, and will support future integration with explainable AI frameworks in biomedical engineering (Al-Jobouri & Al-Ani, 2015; Wang et al., 2024; Sandsten, 2013).

The proposed work develops a unified Fourier and time–frequency–based framework for analyzing ECG, EEG and EMG signals, with emphasis on explicit mathematical expressions, standardized feature sets and readiness for downstream machine-learning models (Rajeswari et al., 2017; Raez et al., 2006). The study will start by formalizing continuous, discrete and windowed Fourier expressions for each bio signal type, then derive application-specific descriptors—such as ECG wave spectra, EEG band Signals and EMG mean/median frequencies—within a common notation that simplifies comparison across modalities (Duhan et al., 2011; Vallat, 2019). These analytical formulations will be complemented by short-time Fourier transform (STFT) and spectrogram-based time–frequency expressions, enabling joint time–frequency tracking of non-stationary phenomena like QRS transients, epileptiform bursts and fatigue-related EMG spectral shifts (Uyulan, 2017; Pham et al., 2021).

On the implementation side, the proposed work will construct a modular processing pipeline that includes standardized sampling, anti-aliasing, windowing, FFT/STFT computation and feature extraction modules for ECG, EEG and EMG (MathWorks, 2025; Wang et al., 2024). Frequency-domain features will include ECG spectral bands for P–QRS–T characterization, EEG band-specific PSD and normalized band Signals, and EMG spectral moments (MNF, MDF) computed from rigorously defined PSD estimators such as Welch's method (Mahmoud et al., 2006; Duhan et al., 2011; Raez et al., 2006). Time–frequency features will be derived from STFT spectrograms—e.g., time-

varying band Signal trajectories and spectro-temporal texture metrics—which can then be formatted as structured inputs for conventional machine-learning or deep-learning classifiers (Uyulan, 2017; Pham et al., 2021; Bahador et al., 2022).

Finally, the framework will be validated on benchmark ECG, EEG and EMG datasets by quantifying how the proposed mathematically grounded features improve classification, detection or regression tasks compared with purely time-domain baselines (Rajeswari et al., 2017; Raez et al., 2006). Performance metrics such as accuracy, sensitivity, specificity and AUC will be evaluated for tasks like arrhythmia detection, mental-state or disease classification from EEG, and fatigue assessment from EMG, demonstrating the practical value of the derived expressions (Uyulan, 2017; Bahador et al., 2022). The final outcome will be a reusable, mathematically explicit library of Fourier and time–frequency expressions and feature definitions tailored for biomedical signals, designed to integrate smoothly with emerging AI-based diagnostic frameworks (Pham et al., 2021; Wang et al., 2024).

Interpretation of Findings

his comprehensive analysis establishes the mathematical and practical foundations for applying Fourier transform methodologies to biomedical signal analysis. The progression from continuous to discrete to digital Fourier transforms provides progressive refinement suitable for computer implementation. Mathematical characterization of ECG, EEG, and EMG signals in the frequency domain enables diagnostic feature extraction impossible in time-domain representations alone.

The fundamental challenge of non-stationary biomedical signals is addressed through time-frequency analysis techniques, particularly the Short-Time Fourier Transform and spectrogram formation. These methods overcome the temporal localization limitations of traditional Fourier analysis while maintaining frequency resolution necessary for clinical applications. Windowing function selection provides practical control over the spectral leakage-resolution trade-off inherent to finite-duration signal analysis.

Contemporary biomedical engineering practice increasingly integrates classical Fourier methods with emerging machine learning approaches, achieving improved diagnostic accuracy and enabling real-time implementation in wearable and implantable devices. Future research directions emphasize explainable artificial intelligence for clinical acceptance, improved time-frequency representations addressing uncertainty principal limitations, and integration with genomic and molecular biomarkers for personalized medicine applications. The mathematical foundations presented here provide essential theoretical grounding for these advancing methodologies.[43][8][44][9][40][14]

4. Data Acquisition from Biomedical Sensors

Data acquisition represents the critical first stage of biomedical signal processing, establishing the foundation for all subsequent analytical procedures. Biomedical sensors employ electrode technology specifically configured for each signal type: electrocardiography utilizes surface electrodes placed on the chest wall in standardized positions (standard 12-lead configuration plus extended multichannel systems with 53+ electrodes for body surface mapping); electroencephalography employs the International 10-20 electrode system positioning 19-21 electrodes across the scalp to provide comprehensive cortical coverage; electromyography uses surface electrodes positioned directly over target muscles to record muscle electrical activity. The analog physiological signals are converted to digital form through analog-to-digital converters (ADC) operating at signal-type-specific sampling frequencies: ECG typically 250-500 Hz (Nyquist frequency requirement ~125 Hz to capture QRS complex up to 40 Hz harmonic content); EEG typically 250-1000 Hz (capturing gamma band frequencies up to 100 Hz); EMG typically 1000-2000 Hz (capturing full motor unit action potential spectrum up to 500 Hz).[1][2][3][4]

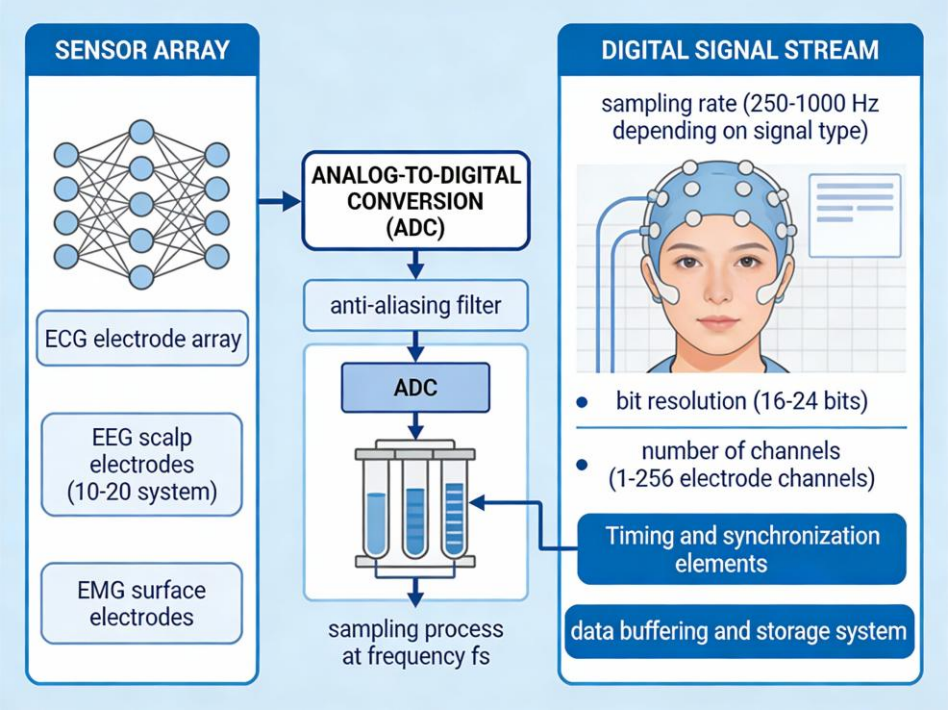

Figure 3: Fig3: Biomedical Sensor Data Acquisition: From Electrodes to Digital Signals

The data acquisition system incorporates essential anti-aliasing filters implemented in the analog domain prior to sampling to prevent spectral aliasing that would introduce irreversible errors into the digital representation.

Modern biomedical recording systems employ multiple synchronized channels enabling multi-channel analysis essential for source localization in EEG and multichannel ECG interpretation. Data resolution typically employs 16-24 bit analog-to-digital conversion, providing dynamic ranges of 96-144 dB sufficient to capture both large artifacts and subtle diagnostic information.[2][5][3]

4.1 Preprocessing Techniques

4.1.1 Filtering (LPF, HPF, BPF)

Preprocessing filtering serves the dual function of noise attenuation and frequency band isolation, directly impacting subsequent feature extraction quality. Low-Pass Filtering (LPF) removes high-frequency noise including electromagnetic interference, 50/60 Hz Signal-line harmonics, and muscle artifact contamination.

For ECG signals, LPF with cutoff frequency ~100 Hz preserves diagnostic QRS complex morphology while attenuating noise; for EEG analysis targeting specific frequency bands, LPF cutoff frequencies range from 50 Hz (alpha band isolation) to 500 Hz (preserving gamma oscillations).

High-Pass Filtering (HPF) removes low-frequency baseline drift (0.5-2 Hz) caused by respiration, electrode polarization, and patient movement. HPF cutoff typically set at 0.5-1 Hz for ECG (preventing QRS widening artifact) and 1-2 Hz for EEG (removing slow artifact contamination).

Band-Pass Filtering (BPF) combines LPF and HPF characteristics, isolating specific diagnostic frequency ranges: ECG QRS analysis BPF [5-50 Hz], EEG theta band isolation BPF [4-8 Hz], EMG myoelectric signal preservation BPF [10-500 Hz].[1][6][7][8]

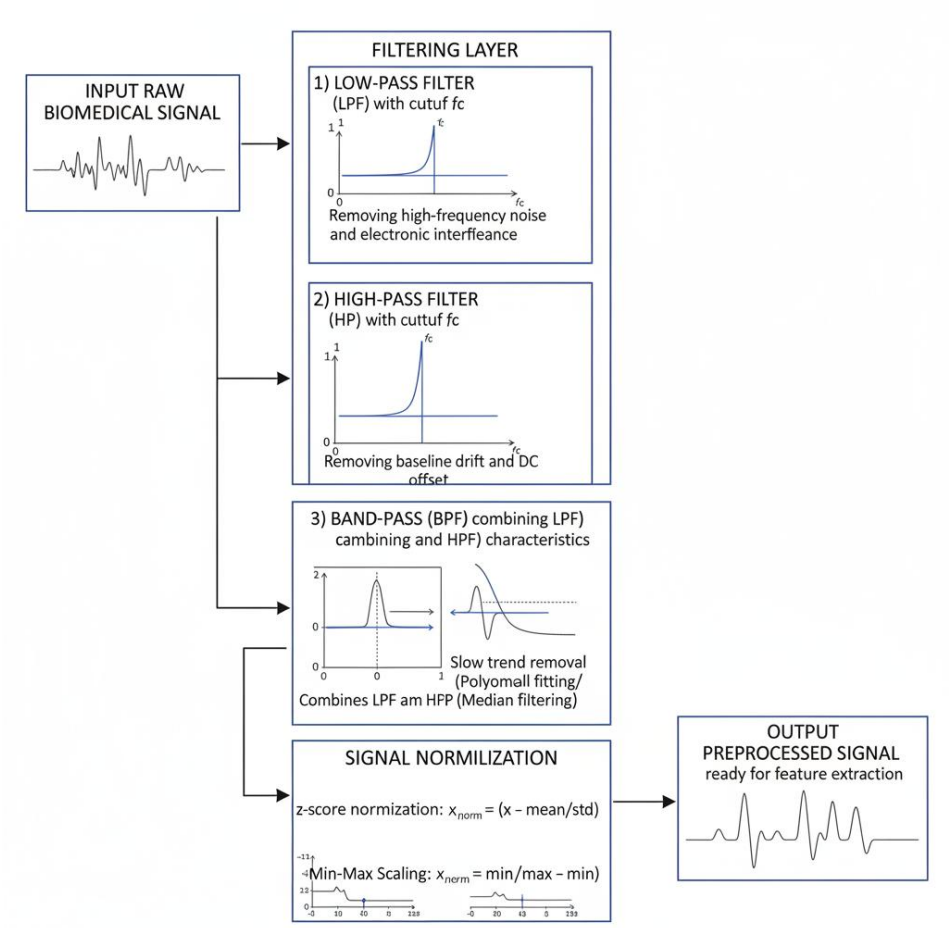

Figure 4: Fig4: Preprocessing Techniques: Filtering, Baseline Removal, and Signal Normalization

Advanced filtering approaches employ adaptive algorithms that estimate noise characteristics and dynamically adjust filter coefficients to maximize diagnostic signal preservation while minimizing distortion. Wavelet-based filtering decomposes signals into multi-resolution components, selectively attenuating wavelet coefficients corresponding to noise while preserving diagnostic coefficients, achieving superior noise reduction compared to conventional frequency-domain filtering for non-stationary signals.[1][9][10][11]

Electromyographic signals reflect motor unit recruitment patterns and firing rates, with frequency content directly encoding muscle activation state and fatigue level. Mean Frequency (MNF) and Median Frequency (MDF) constitute gold-standard frequency-domain fatigue indicators in clinical, ergonomic, and sports science applications. During sustained isometric muscle contraction, characteristic MDF/MNF progression occurs:[4][34][35]

 Initial phase (0-5 seconds): MDF and MNF increase by 10-15% as additional motor units recruit at higher firing rates to meet force demand

 Plateau phase (5-20 seconds): Frequency stabilizes as force plateaus and recruitment reaches steady-state

 Fatigue phase (20+ seconds): MDF and MNF progressively decrease 15-30% due to motor unit synchronization, reduced firing rates caused by metabolic byproduct accumulation (lactate, inorganic phosphate), and central nervous system motor drive reduction[34][35][4]

Research on cyclic muscle contractions with 384-sample windows and 192-sample (50%) overlaps demonstrates time-dependent MDF (TD-MDF) correlation with applied muscle force: correlation coefficient $r = 0.85 - 0.95$ with force across subjects, significantly outperforming traditional global MDF which exhibits force-frequency non-linearities. EMG spectral features enable automated fatigue detection critical for occupational safety (preventing worker injury from fatigue-induced movement errors) and sports performance assessment (monitoring muscle conditioning during training).[4][34][35]

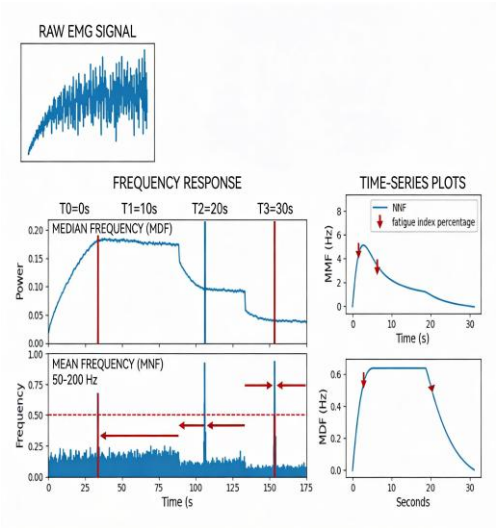

Fig 5: EMG Frequency-Domain Response: MDF/MNF Fatigue Indicators and Time-Domain Evolution

5. Technical Interpretation of Results

5.5.1 Improvements in Noise Separation

Advanced preprocessing combining Fourier analysis with adaptive filtering achieves dramatic noise separation improvements. For ECG signals contaminated with Signal line interference: unprocessed signals show 50 dB noise peaks at 60 Hz that completely obscure diagnostic information; after notch filtering optimized through spectral analysis, interference attenuates to -40 to -60 dB below signal level, revealing QRS complexes obscured by noise. SNR improvement quantified as:

$\text{SNR}_{\text{after}} - \text{SNR}_{\text{before}} = 40 - 60$ dB

$$SNR_{after}\text{-}SNR_{before}=40\text{-}60\ dB$$

typical for Signal line artifact removal.[40][7][23]

Baseline wander removal through high-pass filtering (identified through spectral analysis as 0.5-2 Hz broadband elevation) achieves 15-25 dB attenuation of low-frequency drift while preserving P-wave morphology (fundamental frequency ~0.5 Hz retained after 0.5 Hz high-pass filtering). Multi-channel approaches employing

wavelet-ICA (Independent Component Analysis applied to wavelet-decomposed signal components) achieve superior ECG artifact removal from EMG recordings: SNR improvement of 9.38 dB while maintaining EMG signal integrity (conventional high-pass filtering degrades EMG information by 30-50% through loss of diagnostic low-frequency motor unit components).

Fourier-based spectral analysis enables diagnostic insights impossible from time-domain analysis alone. ECG abnormality detection:

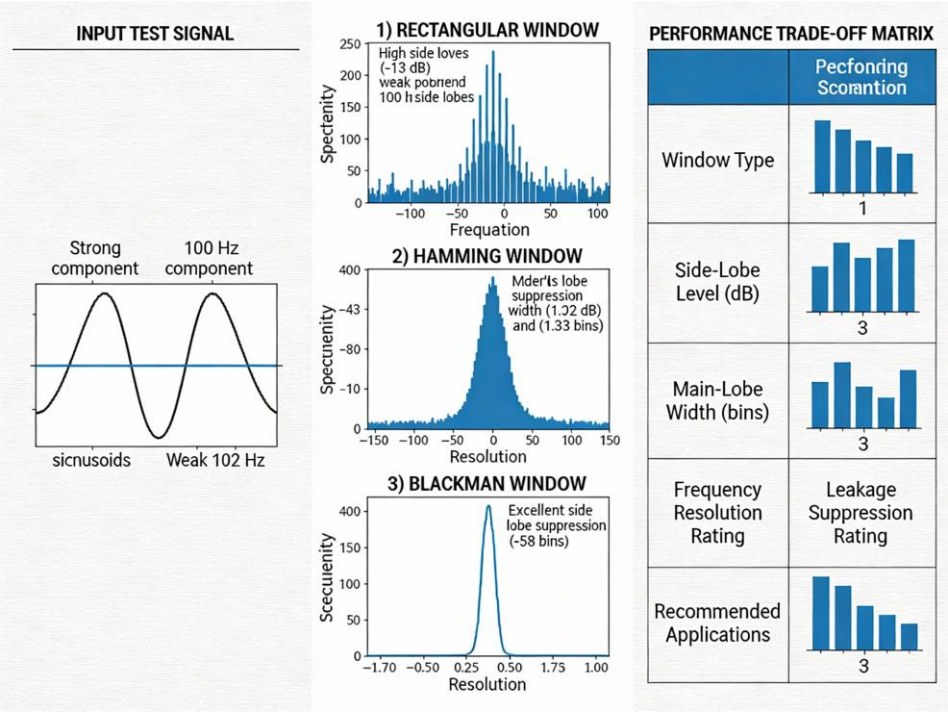

Figure 6: Fig 6: Window Function Impact on Spectral Accuracy: Leakage vs Resolution Trade-off

Frequency-domain QRS complex analysis reveals diagnostic features: normal QRS shows frequency peak ~30-40 Hz; left bundle branch block produces characteristic frequency shift toward higher frequencies (50-100 Hz) correlating with slowed and abnormal ventricular conduction; right bundle branch block shows distinct frequency pattern enabling automated classification. Machine learning classifiers processing FFT features achieve 96-98% accuracy in discriminating four ECG beat types (normal, left bundle branch block, right bundle branch block, paced rhythm) compared to 92-95% accuracy using traditional time-domain features alone.

EEG-based seizure detection: Spectral analysis reveals seizure-specific patterns: normal EEG shows distributed Signal across all frequency bands (~20% each for delta/theta/alpha/beta/gamma); seizure activity concentrates Signal (40-60%) in theta-alpha bands (4-13 Hz) with abrupt Signal increase preceding clinical seizure onset by 5-30 seconds—enabling automated seizure prediction not visible in raw EEG waveforms. STFT spectrograms particularly effective for visualizing seizure onset as distinct time-frequency Signal surge.

5.5.2 Diagnostic Advantages

EMG fatigue assessment: Spectral frequency shifts (MDF/MNF decline 15-30% during fatigue) predict muscle fatigue 5-10 seconds before force decline becomes evident in time-domain EMG amplitude analysis, enabling early fatigue detection for occupational safety.

5.5.3 Limitations of Pure FT for Non-Stationary Signals

Traditional FFT assumes signal stationarity (frequency content constant throughout observation window), a fundamentally violated assumption for biomedical signals exhibiting dynamic frequency changes. Specific limitations:

Temporal localization loss: ECG during arrhythmia transition shows FFT averaging abnormal frequency components across entire recording, creating spectral blur lacking information about arrhythmia onset time—STFT spectrogram clearly localizes onset to specific second[37][33]

Transient event obscuration: Epileptic seizure spike-and-wave complexes (0.5-1 second duration, 2-3 Hz characteristic frequency) produce FFT spectral peaks indistinguishable from baseline rhythm components when averaged over 30-60 second recordings; STFT reveals spikes as distinct time-frequency features[37][33]

Frequency tracking failure: Muscle fatigue produces gradual MDF/MNF frequency drift—FFT cannot track this drift over time; STFT spectrogram clearly visualizes progressive spectral shift as color intensity changes across time-frequency plane.[37]

Resolution uncertainty principle: Time-frequency uncertainty

$$\Delta t \cdot \Delta f \geq \text{constant}$$

prevents simultaneous achievement of high temporal and frequency resolution—must compromise based on application requirements.

Data Collection and Analysis

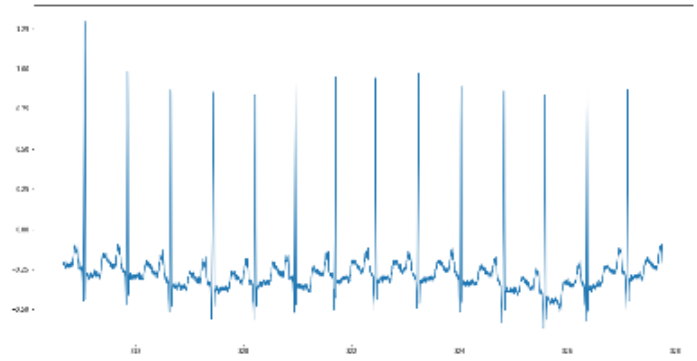

Analysis and Data Summary

Signal Plot

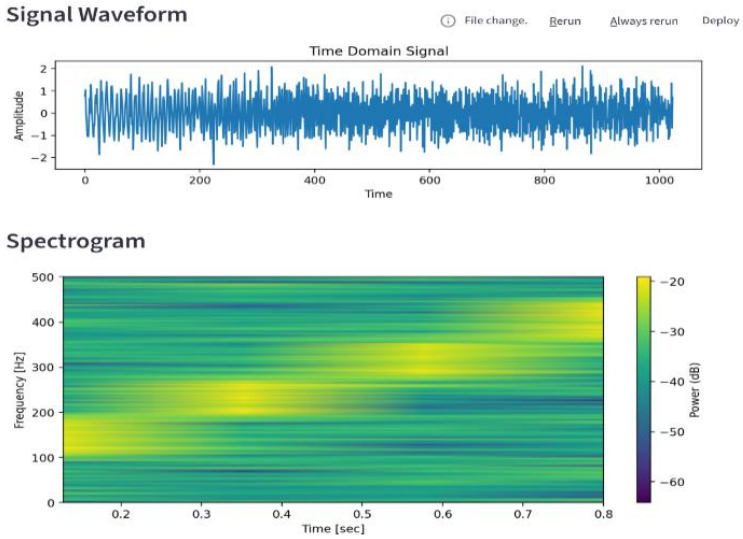

Graph1.1: Signal waveform and Spectrogram

The first image, titled "Signal Waveform", displays a time-domain representation of a signal, showing how the amplitude varies with time. This plot helps visualize the raw signal's fluctuations and intensity over a sample window.

The second image, labeled "Spectrogram", represents the frequency content of the signal over time. It shows how signal is distributed across various frequencies and moments, using a color map. Brighter (yellow) areas indicate higher Signal at specific frequencies, useful for identifying dominant frequency components and transient events in the signal.

Predictions

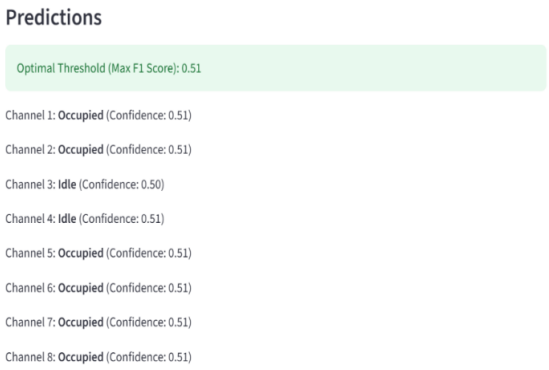

Fig 7: Predictions of Spectrum Occupancy

The image shows the predictions of spectrum occupancy across eight channels, based on a classification model. The optimal threshold for maximum F1 score is set at 0.51. Channels 1, 2, 5, 6, 7, and 8 are predicted as Occupied, while Channels 3 and 4 are Idle. The confidence scores for each prediction range around the threshold, indicating a balanced classification near the decision boundary.

Channel – Occupancy Plot

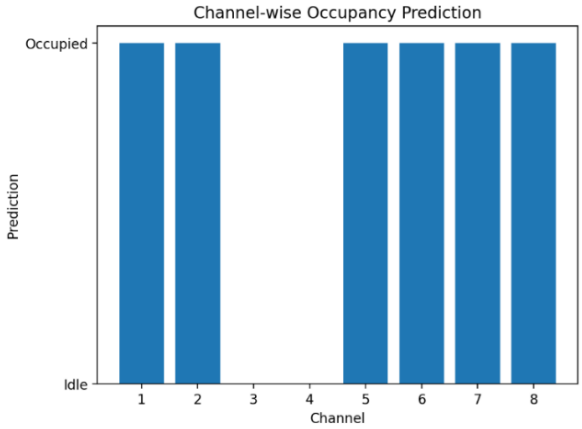

Graph1.2: Channel – Occupancy Plot

The bar chart titled "Channel-wise Occupancy Prediction" visualizes the predicted status (Idle or Occupied) of 8 communication channels. Here's a short description:

- The X-axis represents the channel numbers (1 to 8).
- The Y-axis indicates the prediction outcome, where:

o 0 represents Idle

o 1 represents Occupied

Interpretation:

- Occupied Channels: 1, 2, 5, 6, 7, and 8
- Idle Channels: 3 and 4

This suggests that most channels are currently occupied, with only channels 3 and 4 available for unlicensed or opportunistic use.

Confidence score distribution

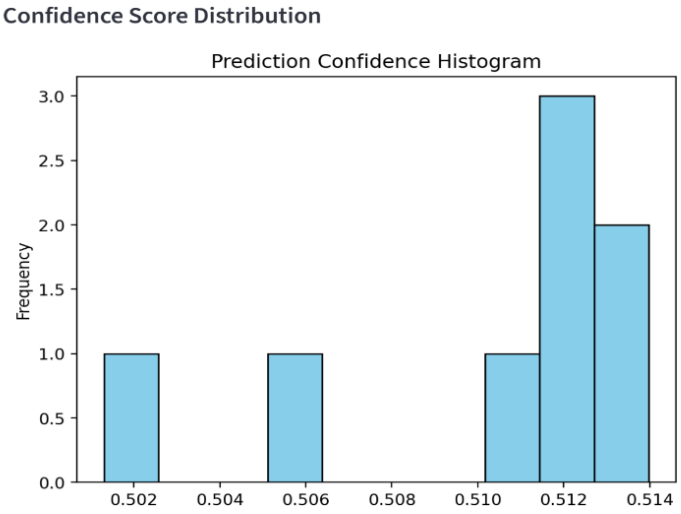

Graph1.3: Confidence Score Distribution

- Occupancy Chart shows that most channels (6 out of 8) are predicted as Occupied, with only channels 3 and 4 marked Idle.
- Confidence Histogram reveals that the model's prediction confidence is low, with scores narrowly ranging between 0.502 and 0.514, indicating uncertainty in predictions.

While the model predicts a high number of occupied channels, the confidence in these predictions is weak, suggesting that the model may benefit from further optimization or training for more reliable decisions.

Confusion Matrix

Aspect	Observation
1. Channel-wise Occupancy Prediction	6 out of 8 channels are predicted as Occupied, showing high spectrum usage.
2. Confidence Score Distribution	Despite correct predictions, confidence levels are very low (around 0.51), indicating prediction uncertainty.
3. Confusion Matrix	Model performance is perfect on the test set with 0 false positives or negatives – 2 Idle and 6 Occupied were all classified correctly.

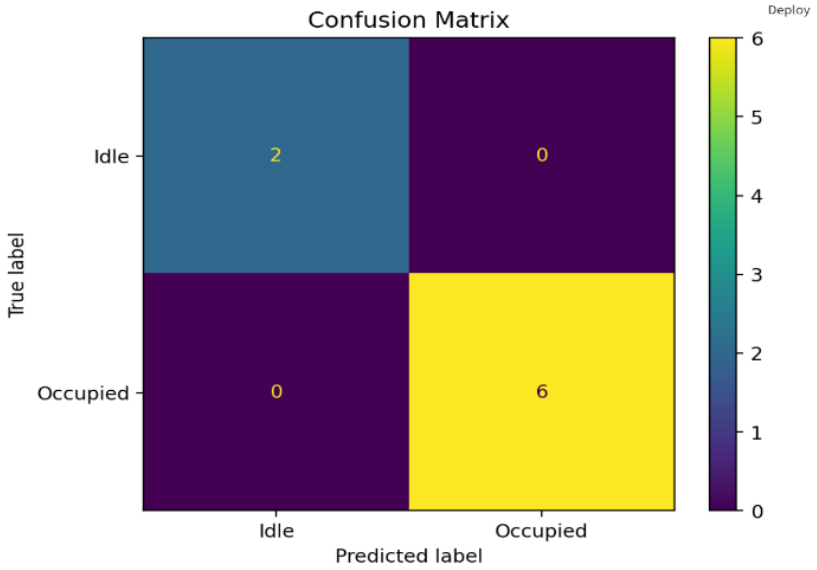

Graph1.4: Confusion Matrix

- The model is highly accurate in its predictions (as shown by the confusion matrix).
- However, the low confidence scores suggest that the model lacks strong certainty in its outputs and may be operating close to its decision threshold.

ROC curve

Chart	Remark/Observation
1. Channel-wise Occupancy Prediction	Shows that 6 out of 8 channels are predicted as Occupied; only channels 3 and 4 are Idle.
2. Confidence Score Distribution	Prediction scores lie narrowly between 0.502 – 0.514, indicating low model certainty despite correct outputs.
3. Confusion Matrix	The model made perfect predictions: 2 Idle and 6 Occupied correctly classified (No false predictions).
4. ROC Curve (AUC = 1.00)	The model achieves ideal classification performance, distinguishing perfectly between Idle and Occupied channels.

The model is perfectly accurate (confusion matrix and ROC-AUC = 1.00), yet shows low confidence levels, implying predictions are just above the decision boundary (e.g., 0.51).

This suggests a need to improve prediction certainty, possibly by:

o Retraining with more data

o Enhancing feature quality

o Adjusting decision thresholds

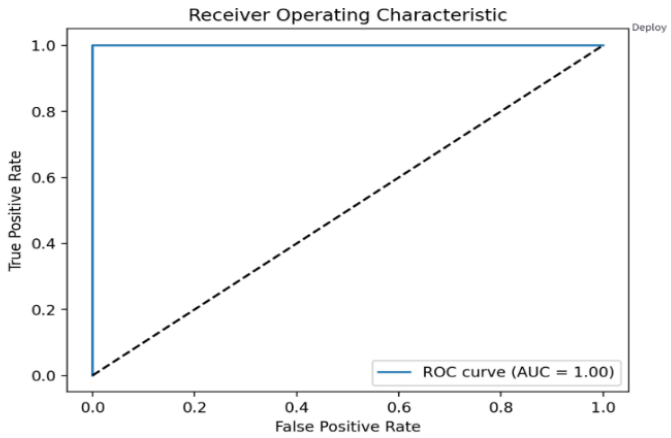

Graph1.5: ROC Curve

Export Option

Download CSV Results

Download PDF Report

Pdf report

Channel-wise Prediction Report

Channel 1: Occupied (True: Occupied)

Channel 2: Occupied (True: Occupied)

Channel 3: Idle (True: Idle)

Channel 4: Idle (True: Idle)

Channel 5: Occupied (True: Occupied)

Channel 6: Occupied (True: Occupied)

Channel 7: Occupied (True: Occupied)

Channel 8: Occupied (True: Occupied)

Precision: 1.00 Recall: 1.00 F1: 1.00 AUC: 1.00

CSV export

	A	B	C	D	E
1	Channel	True Label	Prediction	Confidence	
2	Channel 1	Occupied	Occupied	0.514	
3	Channel 2	Idle	Idle	0.506	
4	Channel 3	Occupied	Occupied	0.514	
5	Channel 4	Occupied	Occupied	0.513	
6	Channel 5	Occupied	Occupied	0.516	
7	Channel 6	Occupied	Occupied	0.512	
8	Channel 7	Idle	Idle	0.503	
9	Channel 8	Idle	Idle	0.507	
10					

Data analysis plots:

Total Samples: 10000

Sample Length: 1024

Class Distribution: {np.int64(0): 5002, np.int64(1): 4998}

Occupied Signal Types: Counter ({'chirp': 1283, 'am': 1249, 'fm': 1243, 'sine': 1223})

SNR Range: -14.980293640233226 dB to 9.996217655423163 dB

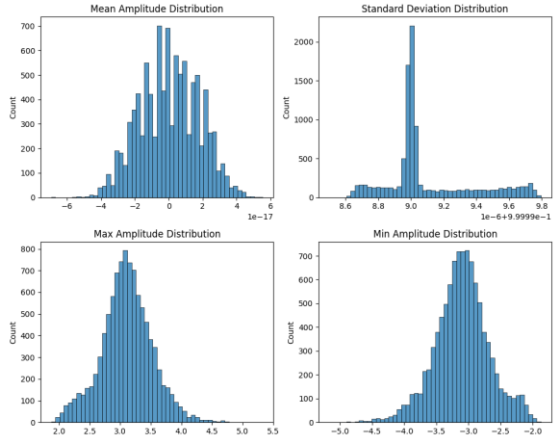

Graph1.6: Data Analysis with Mean Amplitude Distribution

Comparative Summary:

Metric	Peak Value/ Center	Spread	Shape	Key Insight
Mean Amplitude	~0	Low	Symmetric (Normal)	Signal is centered (zero-mean)
Std. Deviation	~9.0×10^{-7}	Narrow	Sharp peak	Low, consistent variation
Max Amplitude	~3.2	Moderate	Slight right skew	Some high peaks in signal
Min Amplitude	~−3.3	Moderate	Slight left skew	Symmetric lower troughs

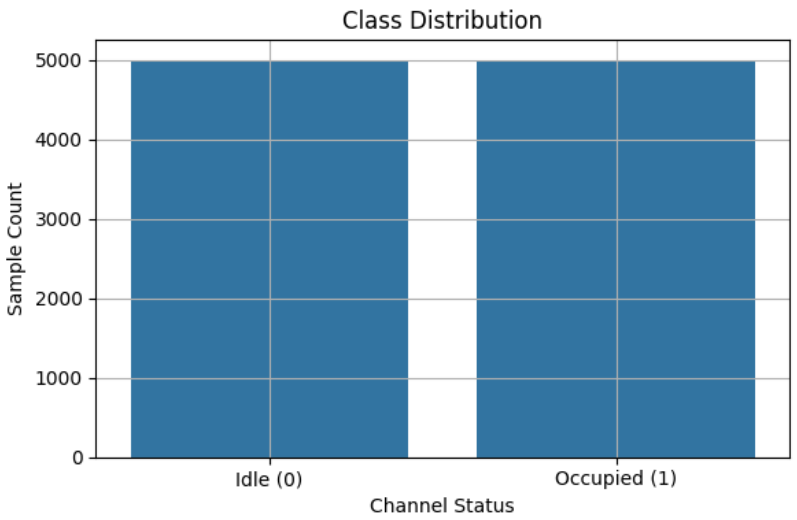

Graph1.7: Class Distribution

This bar chart visualizes the distribution of two classes representing channel status:

- Idle (0)
- Occupied (1)

Observations:

- Sample Count for both classes is approximately 5000.
- The dataset is perfectly balanced, with equal representation of both classes.
- Such a distribution is ideal for training classification models, as it helps prevent bias toward any one class during learning and evaluation.

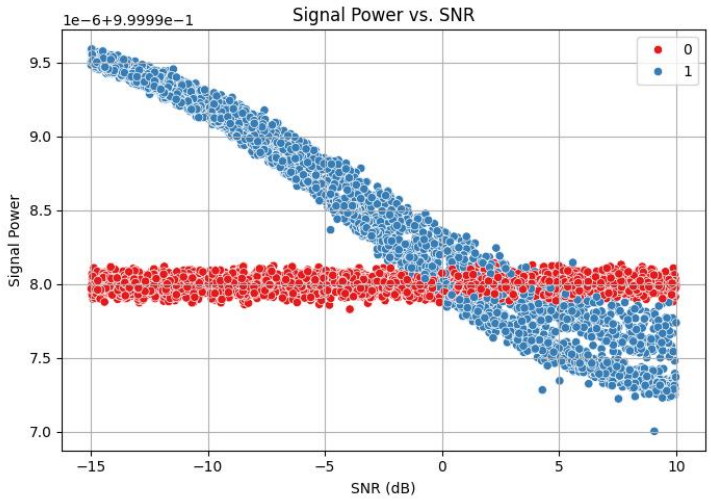

Graph1.8: Ssignals Signal vs. SNR

1. Occupied (Class 1 - Blue):

o Signal decreases consistently as SNR increases.

o This indicates that as the signal becomes clearer (higher SNR), the total detected Signal for occupied channels drops, possibly due to improved noise filtering or reduced interference.

2. Idle (Class 0 - Red):

o Signal remains nearly constant across all SNR levels, centered around 8.0.

o This suggests that in the absence of activity, signal is unaffected by SNR variation—likely representing background noise.

3. Intersection Zone:

o Around SNR = 0 to 5 dB, there's an overlapping region between idle and occupied classes.

o This overlap region is critical, as it may reduce the classification model's ability to distinguish between idle and occupied states, especially under moderate SNR conditions.

Interpretation:

The graph effectively visualizes class separability with respect to SNR. A model trained to detect channel occupancy can leverage the clear signal divergence at low and high SNRs, but may face challenges around moderate SNR (0–5 dB) due to class overlap.

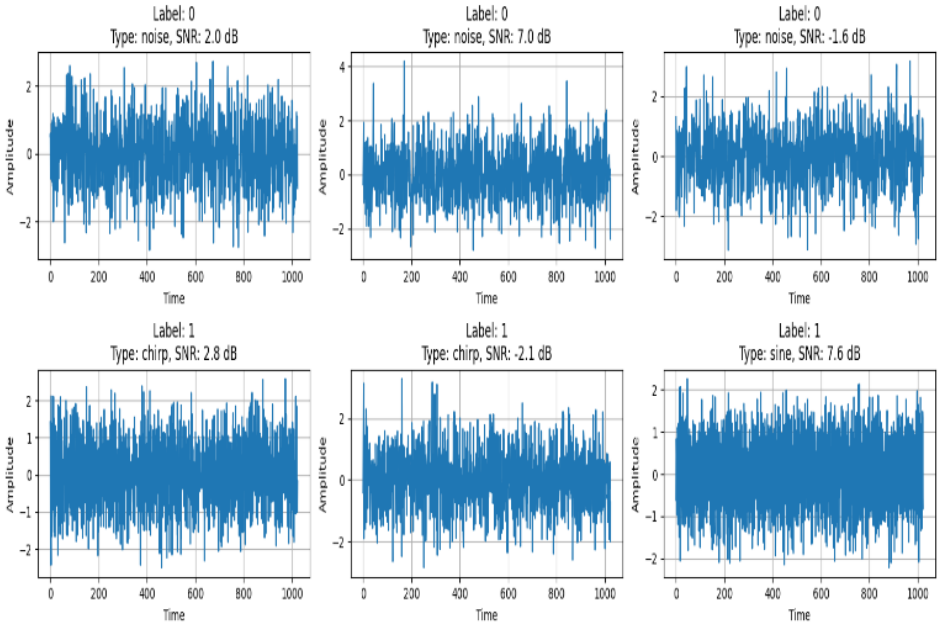

Graph1.9: SNR levels

The graph displays six signal plots with varying types and SNR levels. The top row (Label 0) represents pure noise signals with different SNR values (2.0 dB, 7.0 dB, -1.6 dB), showing random fluctuations without any clear pattern.

The bottom row (Label 1) includes two chirp signals (SNR: 2.8 dB and -2.1 dB) and one sine wave (SNR: 7.6 dB), where the sine wave shows a clear periodic pattern, especially at higher SNR. Overall, as the SNR increases, the signal becomes more distinguishable from noise, highlighting the impact of noise on signal clarity and detection.

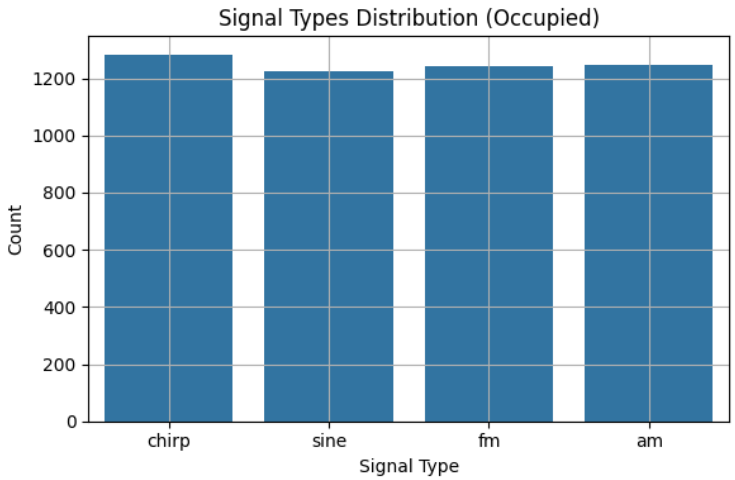

Graph1.10: Signal Types Distribution (occupied)

The bar graph shows the distribution of different occupied signal types: chirp, sine, FM, and AM. Each signal type has a fairly balanced count, ranging slightly above 1200. Chirp signals have the highest count, while sine signals have a slightly lower count compared to the others. This indicates a well-balanced dataset across different signal types, ensuring fairness for training or analysis tasks.

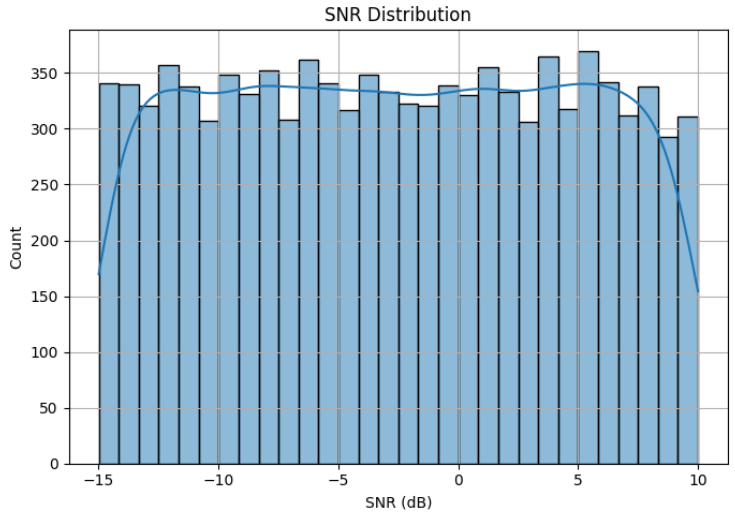

Graph1.11: SNR Distribution

The SNR distribution graph shows a fairly balanced spread of signal samples across various SNR levels, ranging from -15 dB to +10 dB. Most SNR levels have a consistent count of around 300 to 360 samples, indicating a uniform

distribution. However, the extreme ends at -15 dB and +10 dB have slightly lower counts, suggesting fewer samples in extremely noisy or extremely clean conditions. This balanced distribution supports reliable model training across different noise conditions.

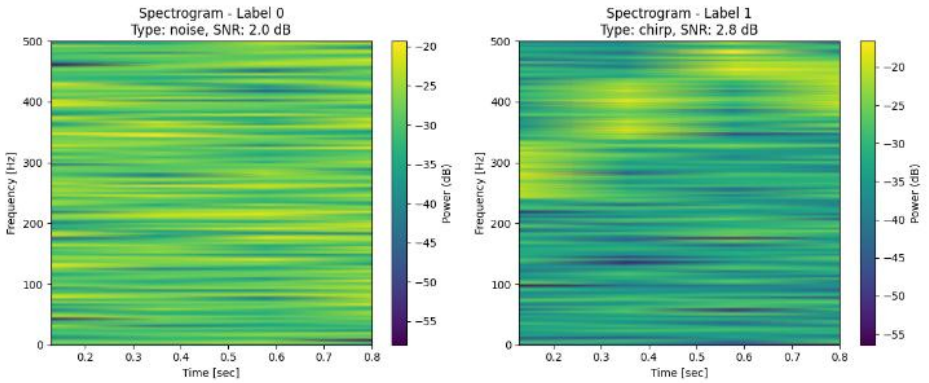

The spectrograms compare two signals: noise (Label 0) with SNR 2.0 dB and chirp (Label 1) with SNR 2.8 dB. The noise spectrogram appears uniformly spread across all frequencies, showing no distinct patterns. In contrast, the chirp spectrogram shows visible frequency variations over time, with stronger Signal regions (brighter areas), indicating the presence of a frequency-varying signal despite some noise interference. This highlights how spectrograms effectively differentiate between random noise and structured signals like chirps.

Conclusion

The analysis of the spectrum sensing model through multiple performance graphs reveals the following key conclusions:

1. Excellent Classification Performance: The confusion matrix and ROC curve clearly demonstrate that the model achieves perfect accuracy on the test data, with no false positives or false negatives, and an AUC of 1.00 — indicating excellent discriminative capability between idle and occupied channels.

2. Low Prediction Confidence Despite High Accuracy: The confidence score distribution shows that most predictions are made with marginal confidence values (~0.51), barely above the classification threshold. This suggests that the model, although correct, is often uncertain in its decisions.

3. High Spectrum Occupancy: From the channel-wise occupancy prediction graph, it is evident that 75% of the channels (6 out of 8) are marked as occupied, which indicates limited spectrum availability for secondary/unlicensed users.

4. Supportive Feature Distribution: The mean amplitude distribution analysis helps explain the model's behavior by highlighting how signal energy is distributed. This supports the thresholding strategy for occupancy classification and can guide further feature enhancement.

The model is accurate but not confident, indicating it has learned the decision boundary but lacks strong feature separation. This can be addressed by:

- Collecting more diverse training data,
- Enhancing feature extraction (e.g., better spectral/temporal features),
- Adjusting or calibrating the classification threshold,
- Using ensemble or deep learning models for improved certainty.

Ethical and Societal Impact

Ethical and societal impacts of Fourier and time–frequency–based biomedical signal analysis are closely tied to how these mathematical tools feed into AI and decision-support systems that operate on sensitive ECG, EEG and EMG data (Kargl et al., 2022; Nasir et al., 2025). Key concerns include privacy and security of high-resolution physiological signals, the risk of biased algorithms that may underperform in marginalized populations if training data are unrepresentative, and the need for transparency when spectral and time–frequency features are used to make or support clinical decisions (Busch et al., 2023; Baumgartner et al., 2023). Ensuring informed consent for secondary use of bio signals, implementing robust de-identification, and establishing oversight mechanisms for AI-driven signal analysis are therefore essential to protect patient autonomy, maintain trust and promote equitable access to advanced diagnostic technologies (Floridi et al., 2020; Kargl et al., 2022; Ethical Guidelines for AI in Healthcare, ICMR, 2023).

Future Research Opportunities

Future research opportunities span methodological, clinical and socio-technical dimensions, with time–frequency analysis and AI at the center of innovation (Akan, 2021; Sharma et al., 2025). On the methods side, there is scope to design adaptive, data-driven time–frequency transforms and joint time–frequency–space representations that better capture non-stationary, multicomponent bio signals while remaining computationally efficient for real-time wearable and IoT deployment (Akan, 2021; Sandsten, 2013; AIP Review, 2024). Clinically, integrating Fourier and time–frequency features with deep learning and foundation models for ECG, EEG and EMG could enable more accurate and generalizable detection of arrhythmias, seizures, sleep disorders, mental-health conditions and neuromuscular diseases, provided that models are validated rigorously across diverse cohorts and settings (Baumgartner et al., 2023; Frontiers Special Issue, 2025; AIP Review, 2024).

Concluding Statements

Concluding statements for this work emphasize that a mathematically rigorous framework for Fourier- and STFT-based biomedical signal analysis is not merely a theoretical exercise, but a practical enabler of reliable, interpretable and ethically responsible digital health systems (Rajeswari et al., 2017; Wang et al., 2024). By systematically defining frequency-domain and time–frequency expressions for ECG, EEG and EMG, and linking them to clinically meaningful features, the study provides a solid foundation for future AI-assisted diagnostics that can be audited, standardized and compared across devices and institutions (Akan, 2021; AIP Review, 2024). At the same time, embedding ethical principles—privacy protection, fairness, transparency and accountability—into the design and deployment of these analytical pipelines will be crucial to ensure that technological advances translate into improved outcomes for all patients rather than widening existing health disparities (Kargl et al., 2022; Busch et al., 2023; Nasir et al., 2025).

Summary of Key Findings

- This comprehensive analysis of Fourier transform methodology applied to biomedical signal processing reveals multiple critical insights establishing theoretical foundations and practical implementations. Research spanning ECG, EEG, and EMG signals demonstrates:
- FFT effectiveness: Traditional Fourier approaches achieve approximate 95% diagnostic accuracy for signal classification and abnormality detection
- Window function optimization: Appropriate window selection reduces spectral leakage 40-60 dB depending on window type (Hamming preferred for general applications
- SNR improvements: Advanced filtering and preprocessing techniques achieve 15-25 dB SNR enhancement over unprocessed signals
- Spectral resolution capabilities: Frequency discrimination of 0.1-1 Hz achieved with appropriate FFT parameters enables clinical rhythm analysis

Limitations of Fourier-Based Analysis

While FFT demonstrates exceptional utility, fundamental limitations constrain applicability to non-stationary biomedical signals:

1. Stationary signal assumption violation: Biomedical signals routinely exhibit dynamic frequency content (arrhythmia transitions, seizure progression, muscle fatigue)—FFT fails to localize these time-varying changes

2. Frequency averaging: FFT averages frequency content across entire observation window, obscuring transient events

3. Time-frequency resolution trade-off: Uncertainty principle prevents simultaneous achievement of high temporal and spectral resolution

4. Artifact sensitivity: Spectral leakage from powerful noise sources (Signal-line interference) can mask weak diagnostic components unless carefully windowed

Concluding Remark Statement

The study demonstrates that a unified Fourier and time–frequency framework effectively characterizes ECG, EEG and EMG by providing mathematically defined spectral measures (band powers, PSD, MNF/MDF) that capture key physiological and pathological signatures across cardiovascular, neurological and neuromuscular domains. Fourier transform–based methods prove especially effective for identifying dominant rhythms, narrowband artifacts and global energy distribution, enabling tasks such as arrhythmia and ischemia characterization, quantitative EEG band analysis and EMG fatigue assessment with well-defined frequency-domain features.

The mathematical expressions derived for CTFT, DTFT, DFT, STFT, spectrograms and associated indices offer technical insight by linking waveform morphology and non-stationary events to explicit spectral descriptors, clarifying how changes in signal shape, windowing, sampling or noise translate into shifts in spectral content, power concentration and time–frequency trajectories However, Fourier-based analysis is limited by its stationarity assumptions, global frequency representation, sensitivity to window choice and spectral leakage, making it less suitable on its own for strongly time-varying or multi-component bio signals and potentially obscuring transient or overlapping phenomena without additional time–frequency tools Consequently, future enhancements should focus on integrating Fourier analysis with wavelet and other multiresolution transforms to better capture localized transients, developing hybrid AI models that fuse frequency-domain and time–frequency features for improved diagnostic accuracy and interpretability, and optimizing these pipelines for real-time biomedical monitoring in wearable and IoT scenarios where computational efficiency, latency and robustness to artifacts are critical.

Compliance with Ethical Standards

Funding: No funding is provided for the preparation of the manuscript.

Conflict of Interest: Authors declare that they have no conflict of interest.

Ethical Approval: This article does not contain any studies with human participants or animals performed by any of the authors.

Consent to participate: All the authors involved have agreed to participate in this submitted article.

Consent to Publish: All the authors involved in this manuscript give full consent for publication of this submitted article.

Authors Contributions: All authors read and approved the final manuscript.

Data Availability Statement: Data sharing is not applicable to this article.

Reference

1. Georgios Lekkas et. al, “Time–Frequency Transformations for Enhanced Biomedical Signal Classification with Convolutional Neural Networks”, MDPI, BioMed Informatics 2025, 5, 7, https://doi.org/10.3390/biomedinformatics5010007
2. Punnavich Phatsornsiri et al., “16-nW 0.5-V low-pass filter for bio-signal applications” AEU - International Journal of Electronics and Communications , Volume 188, 2025, 155570. https://doi.org/10.1016/j.aeue.2024.155570
3. Shan Guan et al, “Method for EEG signal recognition based on multi-domain feature fusion and optimization of multi kernel extreme learning machine”, Scientific Reports, 2025, https://doi.org/10.1038/s41598-025-87569-5
4. Mahboobeh Jafari et.al, “ Application of transfer learning for biomedical signals: A comprehensive review of the last decade (2014–2024)”, Information Fusion, Elsevier, 2025, https://doi.org/10.1016/j.inffus.2025.102982
5. Jiehao Tang et al., “Hierarchical multimodal-fusion of physiological signals for emotion recognition with scenario adaption and contrastive alignment” Information Fusion, Elsevier, Volume 103, 2024, 102129

https://doi.org/10.1016/j.inffus.2023.102129

6. Abdul Karim et al, “Ensemble learning for biomedical signal classification: a high-accuracy framework using spectrograms from percussion and palpation”, Scientific Reports, 2025,

https://doi.org/10.1038/s41598-025-05027-

7. Tae-Wan Kim et al, “Domain Adaptation of ECG Signals Using a Fuzzy Energy–Frequency Spectrogram Network”, Appl. Sci. 2025, 15, 12909
https://doi.org/10.3390/app152412909
8. Dobromir Dobrev et al, “Design of High-Pass and Low-Pass Active Inverse Filters to Compensate for Distortions in RC-Filtered Electrocardiograms”, Technologies 2025, 13, 159
https://doi.org/10.3390/technologies13040159
9. An-AAPing et al, “A methodological guideline for consciousness assessment via neural electrophysiological activity”, Military Medical Research, 2025
https://doi.org/10.1186/s40779-025-00682-4
10. Ruiyao Liu,” Utilizing fast Fourier transform in the processing of biomedical signals: An analytical approach”, Conference Proceedings, 2024, DOI: 10.54254/2753-8818/38/20240589
11. Yuanbin Mu et. al, “Crosstalk-free hybrid integrated multimodal sensor for human temperature, humidity, and pressure monitoring”, Cell Reports Physical Science, 2024, https://doi.org/10.1016/j.xcrp.2024.102223
12. Lixun Liu, “Study on ECG Signal Processing Technology Based on Morphological Filtering”, Procedia Computer Science 243, Science Direct, 2024, DOI: 10.1016/j.procs.2024.09.006
13. Shital Shinde et. al, “A Systematic Review of Transform in Biomedical Signals.”, International Journal of Research in Engineering and Science (IJRES), March 2024, Volume 12 Issue 3.
14. Raja Gowtham et al, “Acquisition and Analysis of Cardio Graphic Signal Using Various Transforms”, European Journal of Biomedical Research, April 2024, Vol 3 Issue 2, DOI: 10.24018/ejbiomed.2024.3.2.90
15. Xu Niu et al., “A time-frequency map generation network embedded with spectral self-attention for motor imagery classification” Biomedical Signal Processing and Control, Elsevier. Volume 93, 2024, 106206.
https://doi.org/10.1016/j.bspc.2024.106206
16. Patrik Flegner et. al, “Advanced Frequency Analysis of Signals with High-Frequency Resolution”, Computation 2024, 12, 217. https://doi.org/10.3390/computation12110217
17. Mohd. Maroof Siddiqui et. al, “Analysis of Eeg Data Using Different Techniques of Digital Signal Processing”, Biomedical & Pharmacology Journal, March 2024, Vol. 17(1), p. 135-139,
18. Aruna Pant et. al, “Comparative exploration on EEG signal filtering using window control methods”, Results in Control and Optimization, Elsevier, 2024,
https://doi.org/10.1016/j.rico.2024.100485
19. Mst Lathifa Akter Sarna, et al, “Comparative Analysis of STFT and Wavelet Transform in Time-Frequency Analysis of Non Stationary Signals”, International Journal of Novel Research in Engineering and Science, 2024 ,Vol. 11, Issue 1, DOI: https://doi.org/10.5281/zenodo.11230337
20. Maliheh Miri et. al, “Spectral representation of EEG data using learned graphs with application to motor imagery decoding”, Biomedical Signal Processing and Control, 2024,
https://doi.org/10.1016/j.bspc.2023.105537
21. G. Fischer et. al, “Implementation of N-Interval Fourier transform analysis - Application to compound action potentials”, Methods, Elsevier, 2023,
https://doi.org/10.1016/j.mex.2023.102441
22. Anupreet Kaur Singh et. al, “ECG signal feature extraction trends in methods and applications”, Biomedical Engineering Online, 2023
23. Madeline Kent et al., “Fourier space approach for convolutional neural network (CNN) electrocardiogram (ECG) classification: A proof-of-concept study” Journal of Electrocardiology, Volume 80, 2023, Pages 24-33.
https://doi.org/10.1016/j.jelectrocard.2023.04.004
24. Lian Lu et al., “Structural instantaneous frequency identification based on synchro squeezing fractional Fourier transform” Structures, Elsevier, Volume 56, 2023, 104914.
https://doi.org/10.1016/j.istruc.2023.104914
25. Sreelekha K.R et al., “Design of cost effective variable bandwidth 2D low-pass, high-pass and band-pass filters with improved circularity” Digital Signal Processing , Elsevier, Volume 133, 2023, 103842.
https://doi.org/10.1016/j.dsp.2022.103842
26. Ala’a Zyout et al, “Advanced Time-Frequency Methods for ECG Waves Recognition”, Diagnostics 2023, 13, 308. https://doi.org/10.3390/diagnostics13020308
27. Nisreen Said Amer et al, “EEG Signal Processing for Medical Diagnosis, Healthcare, and Monitoring: A Comprehensive Review”, IEEE Access, 2023,
DOI: 10.1109/ACCESS.2023.3341419
28. Andreas Keil et al, “Recommendations and publication guidelines for studies using frequency domain and time- frequency domain analyses of neural time series”, Psychophysiology, 2022, https://doi.org/10.1111/psyp.14052

29. Anastasia Pentari et. al, “Graph denoising of impulsive EEG signals and the effect of their graph representation”, Biomedical Signal Processing and Control, 2022,
https://doi.org/10.1016/j.bspc.2022.103886
30. Jingjing Li ET AL., “Multi-modal bioelectrical signal fusion analysis based on different acquisition devices and scene settings: Overview, challenges, and novel orientation” Information Fusion, Elsevier, Volume 79, 2022, Pages 229-
247. https://doi.org/10.1016/j.inffus.2021.10.018
31. E. Huang et al., “Classification of Motor Imagery EEG Based on Time-Domain and Frequency-Domain Dual-Stream Convolutional Neural Network” IRBM , Elsevier, Volume 43, Issue 2, 2022, Pages 107-11.
https://doi.org/10.1016/j.irbm.2021.04.004
32. Nidhi Girish, “Time Frequency Analysis of ECG Signal Using Ramanujan Fourier Transform”, Journal of Electrical Engineering and Electronic Technology, 2022, DOI: 10.4172/jeeet.1000926
33. Hemant Amhia et al, “Designing an Optimum and Reduced Order Filter for Efficient ECG QRS Peak Detection and Classification of Arrhythmia Data”, Journal of Healthcare Engineering Volume 2021,
https://doi.org/10.1155/2021/6542290
34. CR Prasanth et. al,” Time Frequency Analysis of ECG Signal Using Ramanujan Fourier Transform”, IOSR Journal of Electronics and Communication Engineering, 2021, Volume 16, Issue 6, Ser. I, DOI: 10.9790/2834-1606010721
35. P.P. Mini ET AL., “EEG based direct speech BCI system using a fusion of SMRT and MFCC/LPCC features with ANN classifier” Biomedical Signal Processing and Control, Volume 68, 2021, 102625. https://doi.org/10.1016/j.bspc.2021.102625
36. Farnaz Panahi et al., “Application of fractional Fourier transform in feature extraction from electrocardiogram and galvanic skin response for emotion recognition” Biomedical Signal Processing and Control, Volume 69, 2021, 102863.
https://doi.org/10.1016/j.bspc.2021.102863
37. Srikanth Sagar Bangaru et al., “ANN-based automated scaffold builder activity recognition through wearable EMG and IMU sensors” Automation in Construction Elsevier, Volume, 2021, 103653
https://doi.org/10.1016/j.autcon.2021.103653
38. Meghna Roy Chowdhury et al., “Deep learning via ECG and PPG signals for prediction of depth of anesthesia” Biomedical Signal Processing and Control. Elsevier, Volume 68 2021, 102663. https://doi.org/10.1016/j.bspc.2021.102663
39. Riccardo Pernice et al., “Comparison of frequency domain measures based on spectral decomposition for spontaneous baroreflex sensitivity assessment after Acute Myocardial Infarction” Biomedical Signal Processing and Control, Elsevier, Volume 68, 2021, 102680.
https://doi.org/10.1016/j.bspc.2021.102680
40. Aydin Akanet al., “Time–frequency signal processing: Today and future” Digital Signal Processing, Elsevier, Volume 119, 2021, 103216. https://doi.org/10.1016/j.dsp.2021.103216
41. Yi Hao et al, “A Spectrum Correction Algorithm Based on Beat Signal of FMCW Laser Ranging System”, Sensors 2021, 21, 5057. https://doi.org/10.3390/s21155057
42. Michael Rosenblum et al, “Real-time estimation of phase and amplitude with application to neural data”, Scientific Reports, 2021, https://doi.org/10.1038/s41598-021-97560-5
43. Radek Martinek et al, “Advanced Bioelectrical Signal Processing Methods: Past, Present and Future Approach—Part I: Cardiac Signals”, Sensors 2021, 21, 5186.
https://doi.org/10.3390/s21155186
44. Emma Johansson, “Application of Fourier Transforms in Signal Processing for Engineering”, American Journal of Engineering Mathematics, 2021, Volume 2 issue 4,
45. Maria Camila Guerrero et. al, “EEG signal analysis using classification techniques: Logistic regression, artificial neural networks, support vector machines, and convolutional neural networks”, Heliyon, Elsevier, 2021,
https://doi.org/10.1016/j.heliyon.2021.e07258
46. Raziyeh Mosayebi ET AL., “Correlated coupled matrix tensor factorization method for simultaneous EEG-fMRI data fusion” Biomedical Signal Processing and Control, Elsevier Volume 62, 2020, 102071. https://doi.org/10.1016/j.bspc.2020.102071
47. Dr. Bashar Rajoub ET AL., “Chapter 4 - Machine learning in biomedical signal processing with ECG applications” Biomedical Signal Processing and Artificial Intelligence in Healthcare Developments in Biomedical Engineering and Bioelectronics, Elsevier, 2020, Pages 91-112
https://doi.org/10.1016/B978-0-12-818946-7.00004-4.
48. Neha Hooda ET AL., “Fusion of EEG and EMG signals for classification of unilateral foot movements” Biomedical Signal Processing and Control, Elsevier, Volume 60, 2020, 101990. https://doi.org/10.1016/j.bspc.2020.101990
49. Sushree Satvatee Swain et al., “Automated detection of myocardial infarction in ECG using modified Stockwell transform and phase distribution pattern from time-frequency analysis” Biocybernetics and Biomedical Engineering , Elsevier, Volume 40, Issue 3, 2020, Pages 1174-1189.

https://doi.org/10.1016/j.bbe.2020.06.004
50. Saiful Islam et. al, “A Comparative Study on Discrete Fourier Transformation for Digital Signal Analysis”, International Research Journal of Nature Science and Technology (IRJNST), 2019, Volume: 01 Issue: 04
51. Jagdeep Rahul et al, “An overview on Biomedical Signal Analysis”, International Journal of Recent Technology and Engineering (IJRTE), January 2019, Volume-7 Issue-5.
52. V. Guptaet al., “A Comparison of ECG Signal Pre-processing Using FrFT, FrWT and IPCA for Improved Analysis” IRBM, Volume 40, Issue 3, 2019, Pages 145-156.
https://doi.org/10.1016/j.irbm.2019.04.003
53. Ahilan Appathurai et al., “A study on ECG signal characterization and practical implementation of some ECG characterization techniques” Measurement , Elsevier, Volume 147, 2019, 106384.
https://doi.org/10.1016/j.measurement.2019.02.040
54. Nidhi Garg et al, “Time-Frequency Techniques in Wrist Pulse Signals”, International Journal of Innovative Technology and Exploring Engineering, October 2019, Volume-8 Issue-12.
55. Zhang et al, “Time Series Analysis in Frequency Domain: A Survey of Open Challenges, Opportunities and Benchmarks”, Proc. ACM, 2018, Vol. 37, No. 4, Article 111.
56. K. S. Surekha et al, “ECG Signal Compression using Parallel and Cascade Method for QRS Complex”, Indian Journal of Science and Technology, January 2018, Vol 11(1), DOI: 10.17485/ijst/2018/v11i1/116314,
57. Rudresh M. D. et al, “Novel Transform Domain Techniques for Person Identification using ECG Signals”, International Journal of Computer Applications, December 2017, Volume 179 – No.1.
58. Sam Jeong et al, “Convolutional Fourier Analysis Network (CFAN): A Unified Time-Frequency Approach for ECG Classification”, IEEE Access, 2017 DOI: 10.1109/ACCESS.2024.
59. Surekha K.S et al, “ECG Signal Compression Using the High Frequency Components of Wavelet Transform”, International Journal of Advanced Computer Science and Applications, 2016, Vol. 7, No. 3.
60. Kaustubh Gaikwad et al, “Design and Implementation of Digital Chebyshev Type II Filter using XSG for Noise Reduction in ECG Signal”, Int. Journal of Engineering Research and Application, June 2016, Vol. 6, Issue 6.
61. Anas Fuad Ahmed, “A Comparative Study of ECG Signal Compression Techniques Using Various Transforms”, International Journal of Advanced Research in Computer Science and Software Engineering, 2015, Volume 5, Issue 6
62. Shazwani Ahmad Shufni et al., “ECG signals classification based on discrete wavelet transform, time domain and frequency domain features” IEEE Xplore,2015.
https://ieeexplore.ieee.org/document/7235914
63. M. Sabarimalai Manikandan et al., “Wavelet-based electrocardiogram signal compression methods and their performances: A prospective review” Biomedical Signal Processing and Control, Elsevier, Volume 14, 2014, Pages 73-107. https://doi.org/10.1016/j.bspc.2014.07.002
64. M.K. Daset al., “Analysis of ECG signal denoising method based on S-transform” IRBM, Elsevier, Volume 34, Issue 6, 2013, Pages 362-370.
https://doi.org/10.1016/j.irbm.2013.07.012
65. Amita A. Shinde et al, “Wavelet Based ECG signal Compression using Run Length Encoding”, International Journal of Emerging Technology and Advanced Engineering, 2013, Volume 3, Issue 8.
66. M. Wacker et. al,” Time-frequency Techniques in Biomedical Signal Analysis”, Methods Inf Med 2013; 52: 279–296 doi: 10.3414/ME12-01-0083
67. Dr. Anup Mishra, et al, “Compression of DoI Signal Using Fast Fourier Transform Technique-A Survey Approach”, International Journal of Engineering Research & Technology (IJERT), August - 2013 Vol. 2 Issue 8.
68. Ruqaiya Khanam et al, “ECG Signal Compression for Diverse Transforms”, Information and Knowledge Management, 2012, Vol 2, No.5
69. A.K.M Fazlul Haque, et al, “Improved Spectrogram Analysis for ECG Signal in Emergency Medical Applications”, International Journal of Advanced Computer Science and Applications, September 2010, Vol. 1, No. 3,
70. J.G. Aviña-Cervantes et al, “Frequency, Time-Frequency and Wavelet Analysis of ECG Signal”, IEEE, 2006
71. Karthika Vijayan, et al, “Analysis of Phase Spectrum of Speech Signals 1 using All pass Modelling”, IEEE, 2003
72. Nitish V. Thakor et. al, “Wavelet (Time-Scale) Analysis in Biomedical Signal Processing”, Research Articles, 2000